

Immunization and Targeted Destruction of Networks using Explosive Percolation

Pau Clusella,^{1,2} Peter Grassberger,^{3,1} Francisco J. Pérez-Reche,^{1,*} and Antonio Politi¹

¹*Institute for Complex Systems and Mathematical Biology, SUPA, University of Aberdeen, Aberdeen AB24 3UE, United Kingdom*

²*Dipartimento di Fisica, Università di Firenze, via G. Sansone 1, I-50019 Sesto Fiorentino, Italy*

³*JSC, FZ Jülich, D-52425 Jülich, Germany*

(Received 31 March 2016; published 8 November 2016)

A new method (“explosive immunization”) is proposed for immunization and targeted destruction of networks. It combines the explosive percolation (EP) paradigm with the idea of maintaining a fragmented distribution of clusters. The ability of each node to block the spread of an infection (or to prevent the existence of a large cluster of connected nodes) is estimated by a score. The algorithm proceeds by first identifying low score nodes that should not be vaccinated or destroyed, analogously to the links selected in EP if they do *not* lead to large clusters. As in EP, this is done by selecting the worst node (weakest blocker) from a finite set of randomly chosen “candidates.” Tests on several real-world and model networks suggest that the method is more efficient and faster than any existing immunization strategy. Because of the latter property it can deal with very large networks.

DOI: [10.1103/PhysRevLett.117.208301](https://doi.org/10.1103/PhysRevLett.117.208301)

Network robustness is a major theme in complex-systems theory that has attracted much attention in recent years [1]. Two specific problems are immunization of networks against epidemic spreading (of infection diseases, computer viruses, or malicious rumors), and the destruction of networks by targeted attacks. At first sight these two look completely different, but they can actually be mapped onto each other. The key observation is that infections spreading in a population use the network of contacts between hosts for their spread. Accordingly, from the viewpoint of the infection, immunization corresponds to an attack that destroys the network on which it can spread. Vaccination of hosts (network nodes) is often the most effective way to prevent large epidemics. Other strategies include manipulating the network topology [2–4] or introducing heterogeneity in transmission of the infection [5–7].

The main task in both cases is to find those nodes (“blockers”) whose removal is most efficient in destroying connectivity. Important blockers (“superblockers”) are often assumed [8] to be equivalent to “superspreaders,” i.e., the most efficient nodes in spreading information, supplies, marketing strategies, or technological innovations. Identifying superspreaders is the subject of a vast literature [1] but, as pointed out in, e.g., Ref. [9], identifying superblockers is not the same as finding superspreaders. Indeed, a node in a densely connected core is in general a good spreader [10], but it is in general a very poor blocker, since the infection can easily find ways to go around it.

Here we devise a strategy that identifies superblockers. Vaccinating such nodes provides an efficient way to fragment the network and reduce the possibility of large epidemic outbreaks. We focus on “static” immunization, which aims at fragmenting the network before a possible outbreak occurs (“dynamical” immunization strategies

where one tries to contain an ongoing epidemic were studied, for instance, in [11]). In our approach, the network consists of N nodes out of which qN are vaccinated; the rest are left susceptible to the infection. The size of an invasion depends on the fraction q of vaccinated nodes, the type of epidemic (e.g., Susceptible-Infected-Removed or Susceptible-Infected-Susceptible [12]), and its virulence. However, the maximum fraction of nodes infected at any time is always bounded by the relative size $S(q)$ of the largest cluster of susceptible nodes, $\mathcal{G}(q)$. Keeping $S(q)$ as small as possible therefore ensures that epidemic outbreaks of any type are as small as they can be for a vaccination level q [8,13]. For large networks, $N \rightarrow \infty$, the aim of immunization is to fragment them so that $S(q) = 0$ [8]. The immunization threshold q_c is defined as the smallest q -value at which $S(q) = 0$. Although q_c is not well defined for finite N , it can be estimated reliably. Our algorithm deteriorates only when the network is too small (in this case, however, an extensive search of the optimal solution can be performed). In general, the smaller the q_c , the more effective the corresponding strategy, since the epidemic can be prevented by vaccinating a smaller set of nodes.

The identification of superspreaders is in general an NP-complete problem [14], and most likely this is also true for finding superblockers. Therefore, heuristic approaches have to be used. Typically a score is assigned to each node using local [15,16] or global [8,13,17] properties. In contrast to most previous papers, we use an “inverse” [13] strategy. We start from a configuration where all nodes are considered as potentially “dangerous” and are thereby virtually vaccinated ($q = 1$); then, increasingly dangerous nodes are progressively “unvaccinated” (i.e., made susceptible). This is directly related to the concept of explosive

percolation (EP) proposed by Achlioptas *et al.* [18,19]. EP has been discussed in a large number of papers because of its very unusual threshold behavior [20]. It is reminiscent of a wide range of explosive (i.e., strongly discontinuous) phenomena in natural processes like social contagion [21], generalized epidemics [22–24], k -core percolation [25], interdependent networks [26,27], synchronization [28–31], or jamming [32] but so far no application of EP had been proposed. To our knowledge, immunization is the first context where EP is practically used.

Two other ingredients are also essential to make our method fast and efficient. (i) We use two different schemes for $q > q_c$ and $q < q_c$, which both combine local and quasiglobal information. (ii) We use the fast Newman-Ziff algorithm [33] to identify clusters of susceptible nodes. In addition, we use a number of heuristic tricks that are described below.

In the following we test the performance of explosive immunization (EI) for both real-world and model networks. Overall, it gives the smallest values of $S(q)$ (although other strategies may locally perform better for specific q -values). Moreover, it gave in all cases by far the lowest values of q_c compared to all other strategies, except for the very recent message passing algorithms of [34,35]. Following the mainstream in network studies, we focused on $S(q)$, which corresponds to outbreaks starting in $\mathcal{G}(q)$. However, outbreaks can also start in any other cluster. An improved success measure $\tilde{S}(q)$ can be indirectly defined from the average number of infected sites $\langle n_{\text{inf}} \rangle = N \sum_i S_i^2(q) \equiv N \tilde{S}^2(q)$, where $S_i(q)$ denote the sizes of all clusters, ordered from the largest to the smallest one [$S_1(q) \equiv S(q)$]. If this is used, our algorithm turns out to be yet more efficient, and is optimal even when $S(q)$ might suggest that it is not (see Supplemental Material (SM) [36]). In addition, our algorithm is also extremely fast: Its time complexity is linear in N up to logarithms.

The method.—We adopt a recursive strategy. Given a configuration with a mixture of vaccinated and susceptible nodes, m candidates are randomly chosen among the vaccinated ones and the least dangerous (i.e., the weakest blocker) is unvaccinated (we use typically $m \sim 10^3$ [37]). The selection process is based on a node score quantifying its blocking ability. The guiding intuition is that harmless nodes should be identified on the basis of the size of the cluster of susceptible nodes they would join if unvaccinated (these clusters should be kept small) and the local effective connectivity which measures their potential danger if made susceptible. As the relative importance of these two ingredients is significantly different below and above the immunization threshold, we use two different scores. The details of both definitions were obtained by a mix of heuristic arguments and trial and error. They should not be considered as essential, and indeed very similar results were obtained by different *Ansätze* within the same spirit; see [36].

The first score, used in the large- q region, is the sum of two separate contributions,

$$\sigma_i^{(1)} = k_i^{(\text{eff})} + \sum_{\mathcal{C} \in \mathcal{N}_i} (\sqrt{|\mathcal{C}|} - 1). \quad (1)$$

The first term $k_i^{(\text{eff})}$ quantifies the potential danger due to the effective local connectivity. It is determined self-consistently from the bare degree k_i ,

$$k_i^{(\text{eff})} = k_i - L_i - M_i(\{k_j^{(\text{eff})}\}). \quad (2)$$

The number L_i of leaves is subtracted since they do not lead anywhere. The number M_i of strong hubs is subtracted since in our inverse protocol they will likely be vaccinated in case of an epidemic. The analysis of several networks has led us to identify strong hubs in a recursive way as those nodes with $k_i^{(\text{eff})} \geq K$ for a suitably chosen cutoff K . We see that the best results are typically obtained with $K \approx 6$ for many networks, including Erdős-Rényi (ER) networks within a wide range of $\langle k \rangle$ [36]. An example of how $k_i^{(\text{eff})}$ is determined is given in Fig. 1, where all of the above details are shown at work. Notice that, according to Eq. (2), nodes surrounded by hubs may play a minor blocking role for spread and can be left unvaccinated, as compared to nodes without hub neighbors. This idea is similar to the score used in [15], but it is opposite of what is assumed, e.g., in page rank [1] and in the collective influence defined in [8].

The second term on the rhs of Eq. (1) is a q -dependent contribution that takes into account the connectivity of the network beyond the neighbors of node i . It is based on the size of the clusters that would be joined by turning the i th node susceptible: \mathcal{N}_i is the set of all clusters linked to the i th node, while $|\mathcal{C}|$ is the size of cluster \mathcal{C} . A question arises about the weight to give to this contribution. In Ref. [13], where only the nonlocal term was considered, a

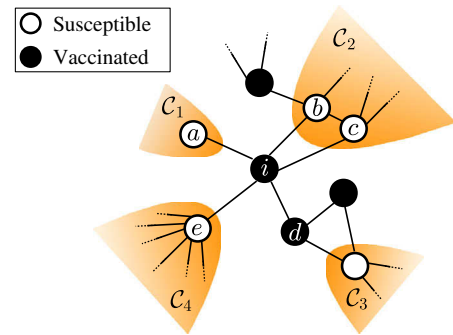


FIG. 1. Illustration of the effective degree $k_i^{(\text{eff})}$ of a generic vaccinated node i . Shaded areas identify distinct clusters of susceptible nodes. With reference to Eq. (2), $k_i = 5$ (see the five neighbors of i labeled $a - e$); only node a is a leaf, so that $L_i = 1$. Assuming that the cutoff K is set equal to 6, none of the nodes $a - d$ is a hub, while node e is a hub provided no more than one of its neighbors is a hub itself.

proportionality to the number $|\mathcal{C}|$ of nodes was assumed; here we find better results by assuming a square root dependence (see also [36]). Additionally, our choice preserves a higher fragmentation, preventing relatively large clusters of susceptibles to merge together. Finally, the nonlocal character of this contribution is better represented by imposing that each addendum is larger than 0 only for clusters containing strictly more than one node: this is the reason for subtracting 1; numerical simulations confirm the validity of this choice.

As we see, using $\sigma_i^{(1)}$ yields small values of q_c . However, it is not suitable to keep a small $S(q)$ below q_c . This is due to the fact that below q_c it leads to big jumps in $S(q)$ when two large clusters join (similar jumps were seen in [13,34,35]). As a result of the merging process, many nodes (at the interface between the two clusters) suddenly become harmless without being treated as such. Accordingly, we use a different score $\sigma_i^{(2)}$ with an even stronger opposition to cluster merging,

$$\sigma_i^{(2)} = \begin{cases} \infty & \text{if } \mathcal{G}(q) \notin \mathcal{N}_i, \\ |\mathcal{N}_i| & \text{else, if } \arg \min_i |\mathcal{N}_i| \text{ is unique,} \\ |\mathcal{N}_i| + \epsilon |\mathcal{C}_2| & \text{else.} \end{cases} \quad (3)$$

Here $|\mathcal{N}_i|$ is the number of clusters in the neighborhood of i , \mathcal{C}_2 is the second-largest cluster in \mathcal{N}_i , and ϵ is a small positive number (its value is not important provided $\epsilon \ll 1/N$). Thus we select only candidates that have the giant cluster in their neighborhood; among these we pick the candidate with the smallest number of neighboring clusters, and if this is not unique, we pick the candidate for which the second-largest neighboring cluster is the smallest (see also [36]). The q -value where the performance of $\sigma_i^{(1)}$ deteriorates depends on the network type and its size. However, we expect the effect to become more pronounced below a value q^* where $S(q^*) \approx 1/\sqrt{N}$, i.e., when a giant cluster starts dominating.

Two remarks are in order about the efficiency of our algorithm. (i) In [13] all vaccinated nodes were considered as candidates to become susceptible during the deimmunization process. This makes the algorithm very slow and prevents its use for large networks. In our tests already $m = 10$ candidates gave very good results, and using $m = 1000$ candidates led to no noticeable degradation [36]. (ii) When joining clusters, we used the very fast Newman-Ziff percolation algorithm [33] that has time complexity $O(N)$ for networks with bounded degrees. It also gives, at each moment, the size of the largest cluster, whose determination would otherwise need most of the CPU time. As a result, we could analyze networks with 10^8 nodes within hours on normal workstations.

Numerical results.—As a first test we studied ER networks with average degree $\langle k \rangle = 3.5$ (to compare with

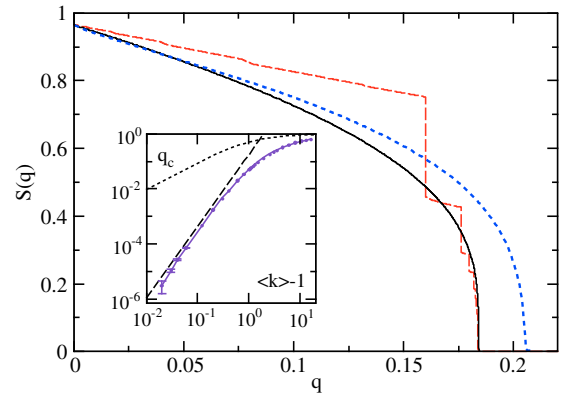


FIG. 2. Relative size $S(q)$ of the largest clusters against q , for ER networks with $N = 10^6$ and $\langle k \rangle = 3.5$. The dashed curve with jumps is obtained, if EI is used with score $\sigma_i^{(1)}$ for all q , 2000 candidates, and $K = 6$. The continuous curve is obtained with $\sigma_i^{(2)}$ for $q < q^*$, where $S(q^*) = 1/500$. The dotted line shows the result from [8]. The inset shows a log-log plot of q_c against $\langle k \rangle - 1$. The straight line indicates the power law $q_c \sim (\langle k \rangle - 1)^{2.6}$, while the dotted curve shows the result for random immunization.

results from [8]). Overall, the best results are obtained by using the scores given in Eqs. (1) and (3) (Fig. 2, solid line in main plot). The dashed line is obtained by using $\sigma_i^{(1)}$ for all q (the big jumps, which were also seen in [13], correspond to joinings of big clusters). It is in general worse than the continuous curve, except close to the jumps (see, however, SM [36]). Finally we show in Fig. 2 also the results obtained with the recently proposed collective influence algorithm [8], which was hailed in as “perfect” [38]. They are significantly worse. Our estimate $q_c \leq 0.1838(1)$ is also smaller than the best estimate $0.192(9)$ obtained in [8] using extremal optimization [39], and used there as a “gold standard” for small networks (it is too slow to be used for large networks).

As regards ER networks with other values of $\langle k \rangle$, we first looked at $\langle k \rangle = 4$, since this had been used in [13]. Our results are similar to those of [13], but significantly better. Next we estimated q_c for a wide range of $\langle k \rangle$. By using networks with N up to 2^{24} we were able to obtain precise results even for $\langle k \rangle$ very close to the threshold $\langle k \rangle = 1$ for the existence of a giant cluster. The results, shown in the inset of Fig. 2, suggest that q_c satisfies for small $\langle k \rangle$ a power law

$$q_c \sim (\langle k \rangle - 1)^{2.6}, \quad (4)$$

where the error of the exponent is $\approx \pm 0.2$. This should be compared to random immunization [40], $q_c^{\text{rand}} = (\langle k \rangle - 1)/\langle k \rangle$ (dotted curve in the inset of Fig. 2). The difference in the exponents reflects the fact that a nearly critical cluster can be destroyed by removing a few “hot” nodes, whence targeted attacks become more efficient as $\langle k \rangle$ approaches the threshold.

Surprisingly, for all $\langle k \rangle$ values except very close to 1, best results are obtained with $K = 6$. This suggests that most nodes with $k_i^{(\text{eff})} > 6$ are vaccinated at q_c , independently of the average degree. This was also verified directly: Although there is no strict relationship between effective degree and blocking power (some hubs were not vaccinated at q_c , while some nodes that were vaccinated are not strong hubs), there is a very strong correlation, stronger than between actual degree and blocking power [36]. On the other hand, very few nodes with small $k_i^{(\text{eff})}$ have to be vaccinated [about 1 per mille of the nodes with $k_i^{(\text{eff})} = 3$], in contrast to claims in [8] that weakly connected nodes are often important blockers.

Scale-free networks.—EI also gives excellent results for scale-free (SF) networks with node degree distribution $p_k \sim k^{-\gamma}$, built with both the Barabási-Albert method (fixed $\gamma = 3$) and the configuration model (γ can be tuned) [1,41]. Our results are significantly better than those obtained with the method from [8] for both settings [Figs. 3(a) and 3(b)]. Using a single score across the entire q -range gives again the best estimate for q_c , while the two-score strategy proves generally superior for $q < q_c$. The jumps obtained in the single-score strategy are less pronounced for the configuration model (and thus the two-score strategy seems less preferable), but the superiority of the two-score strategy becomes again clear when using the improved $\tilde{S}(q)$ discussed in [36].

Observe that the shape of $S(q)$ near $q = 0$ is concave (convex) for large (small) γ [compare panels (a) and (b) in Fig. 3]. The convex shape for small γ is due to the presence of many hubs that lead to a drastic decrease of $S(q)$ when vaccinated at small q .

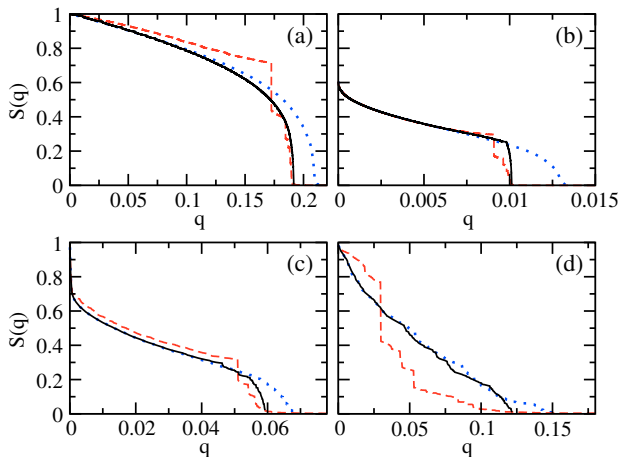


FIG. 3. Relative size $S(q)$ of the largest clusters in SF networks of size $N = 10^6$ obtained with (a) the Albert-Barabási model ($\gamma = 3$) and (b) the configuration model with $\gamma = 2.5$. Panels (c) and (d) show results for the cattle and airport transportation networks, respectively. Different line types correspond to different algorithms: EI using scores $\sigma_i^{(1)}$ and $\sigma_i^{(2)}$ (continuous line) or only score $\sigma_i^{(1)}$ (dashed line) and the algorithm in [8] (dotted line).

Real-world networks.—We have also studied the performance of EI on a number of real-world networks, starting from an example in which immunization plays an important role for food security [42,43]: a network of Scottish cattle movements [44]. The network consists of $N = 7228$ premises (nodes) connected by $E = 24784$ transportation events (edges) occurring between 2005 and 2007. The node distribution obeys a power law with exponent $\gamma = 2.37 \pm 0.06$ (maximum likelihood fit). The scenario is similar to that of SF networks with small γ [compare panels (c) and (b) in Fig. 3]. Again, $S(q)$ decreases quite quickly because of the presence of many well-connected nodes (e.g., markets and slaughterhouses), whose immunization leads to a drastic decrease of the largest cluster. Once again we see that our strategy using two scores is superior to the previous approaches.

We have also studied several networks that were used as the benchmark in previous works. This includes the high-energy physicist collaboration network [45] and the Internet at autonomous system level [46]. In both cases our results are similar to, but slightly better than, those in [13] (which were the best previous estimates). The results for these and soil networks [47] are shown in [36].

A particularly problematic case is the airline network [48], also studied in [2]. This is a rather small network ($N = 3151$ and $E = 27158$) with a broad degree distribution (power law with $\gamma = 1.70 \pm 0.04$). The results reported in Fig. 3(d) show that $\sigma_i^{(1)}$ provides very low $S(q)$ almost everywhere. We conjecture that this is due to the unusually small γ , which implies an abundant number of hubs. As a result, the outcome of the score $\sigma_i^{(2)}$ strongly depends on the value of q_c that is selected. It is anyway clear that a suitable combination of them provides the optimal results.

Conclusions.—In this paper, we extend the explosive percolation concept to propose a two-score strategy for attacking networks that proves superior to all previously proposed protocols. The comparison between the two scores suggests that an everywhere optimal strategy using a single score is unlikely to exist. This is to be traced back to the NP completeness of the problem. Since immunization of a network by vaccinating nodes can be regarded as a strategy for destroying the network on which an infection can propagate, this also gives a nearly optimal strategy for immunization. Our explosive immunization method seems superior, both as regards speed and minimal cost (as measured by the number of vaccinated nodes) to all previous strategies.

We have focused on immunization of nodes but EI can also be applied to immunization of links. This would provide nearly optimal quarantine strategies that might significantly improve the typical brute-force implementation that cuts all the links between two parts of a network. Targeted removal of links with high betweenness centrality is the basis for one of the most efficient algorithms for finding network communities [49]. We propose that

explosive immunization of links should also provide a very efficient algorithm for community detection.

The authors acknowledge financial support from the Leverhulme Trust (Grant No. VP2-2014-043) and from Horizon2020 (Grant No. 642563 - COSMOS).

*Corresponding author.

fperez-reche@abdn.ac.uk

- [1] M. E. J. Newman, *Networks: An Introduction* (Oxford University Press, Oxford, 2010).
- [2] C. M. Schneider, T. Mihaljev, S. Havlin, and H. J. Herrmann, *Phys. Rev. E* **84**, 061911 (2011).
- [3] C. M. Schneider, N. Yazdani, N. A. M. Araújo, S. Havlin, and H. J. Herrmann, *Sci. Rep.* **3**, 1969 (2013).
- [4] A. Zeng and W. Liu, *Phys. Rev. E* **85**, 066130 (2012).
- [5] F. J. Pérez-Reche, S. N. Taraskin, L. da F. Costa, F. M. Neri, and C. A. Gilligan, *J. R. Soc. Interface* **7**, 1083 (2010).
- [6] F. M. Neri, F. J. Pérez-Reche, S. N. Taraskin, and C. A. Gilligan, *J. R. Soc. Interface* **8**, 201 (2011).
- [7] F. M. Neri, A. Bates, W. S. Fuchtbauer, F. J. Pérez-Reche, S. N. Taraskin, W. Otten, D. J. Bailey, and C. A. Gilligan, *PLoS Comput. Biol.* **7**, e1002174 (2011).
- [8] F. Morone and H. A. Makse, *Nature (London)* **524**, 65 (2015).
- [9] Habiba, Y. Yu, T. Y. Berger-Wolf, and J. Saia, Finding Spread Blockers in Dynamic Networks, in *Advances in Social Network Mining and Analysis* (Springer, Berlin Heidelberg, 2010), pp. 55–76.
- [10] S. Pei and H. A. Makse, *J. Stat. Mech.: Theory Exp.* **2013**, P12002 (2013).
- [11] Q. Wu, X. Fu, Z. Jin, and M. Small, *Physica (Amsterdam)* **419A**, 566 (2015).
- [12] L. Hébert-Dufresne, A. Allard, J.-G. Young, and L. J. Dubé, *Sci. Rep.* **3**, 2171 (2013).
- [13] C. M. Schneider, T. Mihaljev, and H. J. Herrmann, *Europhys. Lett.* **98**, 46002 (2012).
- [14] D. Kempe, J. Kleinberg, and É. Tardos, Maximizing the spread of influence through a social network, in *Proceedings of the Ninth ACM SIGKDD Int. Conf. Knowl. Discov. Data Min.—KDD, 2003* (ACM Press, New York, 2003), p. 137.
- [15] Y. Liu, Y. Deng, and B. Wei, *Chaos* **26**, 013106 (2016).
- [16] P. Holme, *Europhys. Lett.* **68**, 908 (2004).
- [17] P. Holme, B. J. Kim, C. N. Yoon, and S. K. Han, *Phys. Rev. E* **65**, 056109 (2002).
- [18] D. Achlioptas, R. M. D'Souza, and J. Spencer, *Science* **323**, 1453 (2009).
- [19] At variance with Ref. [18], where bond percolation has been explored, here, it is more natural to deal with site percolation: this is, however, a minor difference.
- [20] A. A. Saberi, *Phys. Rep.* **578**, 1 (2015).
- [21] J. Gómez-Gardeñes, L. Lotero, S. N. Taraskin, and F. J. Pérez-Reche, *Sci. Rep.* **6**, 19767 (2016).
- [22] H.-K. Janssen, M. Müller, and O. Stenull, *Phys. Rev. E* **70**, 026114 (2004).
- [23] G. Bizhani, M. Paczuski, and P. Grassberger, *Phys. Rev. E* **86**, 011128 (2012).
- [24] K. Chung, Y. Baek, D. Kim, M. Ha, and H. Jeong, *Phys. Rev. E* **89**, 052811 (2014).
- [25] S. N. Dorogovtsev, A. V. Goltsev, and J. F. F. Mendes, *Phys. Rev. Lett.* **96**, 040601 (2006).
- [26] S. V. Buldyrev, R. Parshani, G. Paul, H. E. Stanley, and S. Havlin, *Nature (London)* **464**, 1025 (2010).
- [27] S.-W. Son, G. Bizhani, C. Christensen, P. Grassberger, and M. Paczuski, *Europhys. Lett.* **97**, 16006 (2012).
- [28] J. Gomez-Gardenes, S. Gomez, A. Arenas, and Y. Moreno, *Phys. Rev. Lett.* **106**, 128701 (2011).
- [29] I. Leyva, R. Sevilla-Escoboza, J. M. Buldu, I. Sendina-Nadal, J. Gomez-Gardenes, A. Arenas, Y. Moreno, S. Gomez, R. Jaimes-Reategui, and S. Boccaletti, *Phys. Rev. Lett.* **108**, 168702 (2012).
- [30] A. E. Motter, S. A. Myers, M. Anghel, and T. Nishikawa, *Nat. Phys.* **9**, 191 (2013).
- [31] P. Ji, T. K. DM. Peron, P. J. Menck, F. A. Rodrigues, and J. Kurths, *Phys. Rev. Lett.* **110**, 218701 (2013).
- [32] P. Echenique, J. Gómez-Gardeñes, and Y. Moreno, *Europhys. Lett.* **71**, 325 (2005).
- [33] M. E. J. Newman and R. M. Ziff, *Phys. Rev. E* **64**, 016706 (2001).
- [34] A. Braunstein, L. Dall'Asta, G. Semerjian, and L. Zdeborová, *arXiv:1603.08883*.
- [35] S. Mugisha and H.-J. Zhou, *arXiv:1603.05781*.
- [36] See Supplemental Material <http://link.aps.org/supplemental/10.1103/PhysRevLett.117.208301> for further details on methods and results.
- [37] Notice that $m = 2$ was used in [18], in the context of EP.
- [38] I. A. Kovács and A.-L. Barabási, *Nature (London)* **524**, 38 (2015).
- [39] S. Boettcher and A. G. Percus, *Phys. Rev. Lett.* **86**, 5211 (2001).
- [40] R. Cohen, K. Erez, D. ben-Avraham, and S. Havlin, *Phys. Rev. Lett.* **86**, 3682 (2001).
- [41] A.-L. Barabási and R. Albert, *Science* **286**, 11 (1999).
- [42] M. J. Keeling, M. E. J. Woolhouse, R. M. May, G. Davies, and B. T. Grenfell, *Nature (London)* **421**, 136 (2003).
- [43] R. R. Kao, D. M. Green, J. Johnson, and I. Z. Kiss, *J. R. Soc. Interface* **4**, 907 (2007).
- [44] Data provided by AHVLA RADAR. The network can be downloaded from <http://link.aps.org/supplemental/xxx>.
- [45] Data downloaded from <http://vlado.fmf.uni-lj.si/pub/networks/data/hep-th/hep-th.htm>.
- [46] Data downloaded from <http://www.netdimes.org> for the year 2012.
- [47] F. J. Pérez-Reche, S. N. Taraskin, W. Otten, M. P. Viana, L. da F. Costa, and C. A. Gilligan, *Phys. Rev. Lett.* **109**, 098102 (2012).
- [48] Data from the OpenFlights Airports Database (<http://openflights.org/data.html>) on 2009.
- [49] M. Girvan and M. E. Newman, *Proc. Natl. Acad. Sci. U.S.A.* **99**, 7821 (2002).